H_0 tension and the string swampland

Luis A. Anchordoqui,[1,2,3] Ignatios Antoniadis,[4,5] Dieter Lüst,[6,7] Jorge F. Soriano,[1,2] and Tomasz R. Taylor[8]

[1]*Department of Physics and Astronomy, Lehman College, City University of New York, New York 10468, USA*
[2]*Department of Physics, Graduate Center, City University of New York, New York 10016, USA*
[3]*Department of Astrophysics, American Museum of Natural History, New York 10024, USA*
[4]*Laboratoire de Physique Théorique et Hautes Énergies - LPTHE Sorbonne Université, CNRS, 4 Place Jussieu, 75005 Paris, France*
[5]*Albert Einstein Center, Institute for Theoretical Physics University of Bern, Sidlerstrasse 5, CH-3012 Bern, Switzerland*
[6]*Max–Planck–Institut für Physik, Werner–Heisenberg–Institut, 80805 München, Germany*
[7]*Arnold Sommerfeld Center for Theoretical Physics Ludwig-Maximilians-Universität München, 80333 München, Germany*
[8]*Department of Physics, Northeastern University, Boston, Massachusetts 02115, USA*

(Received 13 December 2019; accepted 14 April 2020; published 23 April 2020)

We realize the Agrawal-Obied-Vafa (AOV) swampland proposal of fading dark matter by the model of Salam-Sezgin and its string realization of Cvetič-Gibbons-Pope. The model describes a compactification of 6-dimensional supergravity with a monopole background on a 2-sphere. In 4 dimensions, there are 2 scalar fields, X and Y, and the effective potential in the Einstein frame is an exponential with respect to Y times a quadratic polynomial in the field e^{-X}. When making the volume of the 2-sphere large, namely for large values of Y, there appears a tower of states, which according to the infinite distance swampland conjecture becomes exponentially massless. If the standard model fields are confined on Neveu-Schwarz 5-branes the 6-dimensional gauge couplings are independent of the string dilaton in the string frame, and upon compactification to 4 dimensions the 4-dimensional gauge couplings depend on X (rather than the dilaton Y) which is fixed at the minimum of the potential. This avoids direct couplings of the dilaton to matter suppressing extra forces competing with gravity. We show that this set up has the salient features of the AOV models, and ergo can potentially ameliorate the tension between local distance ladder and cosmic microwave background estimates of the Hubble constant H_0. Indeed, the tower of string states that emerges from the rolling of Y constitutes a portion of the dark matter, and the way in which the X particle and its Kaluza-Klein excitations evolve over time (refer to as fading dark matter) is responsible for reducing the H_0 tension. Although the AOV proposal does not fully resolve the tension in H_0 measurements, it provides a dynamical dark energy model of cosmology that satisfies the de Sitter swampland conjecture. We comment on a viable solution to overcome the tension between low- and high-redshift observations within the AOV background and discuss the implications for the swampland program.

DOI: 10.1103/PhysRevD.101.083532

I. INTRODUCTION

Over the past decade or so, and through many experiments, it has become indisputable that cosmological observations favor an effective de-Sitter (dS) constant H that nearly saturates the upper bound given by the present-day value of the Hubble constant, H_0. The ΛCDM model, in which the expansion of the universe today is dominated by the cosmological constant Λ and cold dark matter (CDM), is the simplest model that provides a reasonably good account of all the data. However, various discrepancies have persisted. In particular, with the increase in precision of recent cosmological datasets, measurements of H_0 provided by high- and low-redshift observations started to be in tension [1]. In the front row, separate determinations of H_0 at low-redshift, including those from Cepheids and Type-Ia supernovae (SNe), point to $H_0 = 74.03 \pm 1.42\ \mathrm{km\,s^{-1}\,Mpc^{-1}}$ [2–7]. Far from it, when the sound horizon is calibrated using data from baryon acoustic oscillations (BAO) and the all-sky map from the temperature fluctuations on the cosmic microwave background (CMB), the inferred value of the Hubble constant within

ΛCDM is $H_0 = 67.4 \pm 0.5\ \mathrm{km\,s^{-1}\,Mpc^{-1}}$ [8–11]. The discrepancy with the latest SH0ES estimate of $H_0 = 74.03 \pm 1.42\ \mathrm{km\,s^{-1}\,Mpc^{-1}}$ [7] is significant at 4.4σ level [7,11], and systematic effects do not seem to be responsible for this inconsistency [12–16]; see however [17].

Among the many possible explanations of the H_0 tension, those connecting this discrepancy to the swampland program stand out. The objective of this program is to extract a set of relatively simple quantitative requirements for low-energy effective field theories that admit a UV completion to a consistent theory of quantum gravity [18]. By now, various swampland conjectures have been proposed [19–34]; for reviews see [35,36]. Of particular interest here is the distance swampland conjecture that can be expressed by the following statement: If a scalar field, coupled to gravity with reduced Planck mass $M_{\rm Pl} = (8\pi G)^{-1/2}$, transverses a trans-Planckian range in the moduli space, a tower of string states becomes light exponentially with increasing distance [20,21,28,37–39]. The exponentially large number of massless string states saturate the covariant entropy bound in an accelerating universe [40,41], and force the scalar field to satisfy the so-called de Sitter swampland conjecture [28]: The gradient of the potential V of a canonically normalized scalar field in a consistent gravity theory must satisfy either the bound, $M_{\rm Pl}|\nabla V| \geq cV$ or must satisfy $M_{\rm Pl}^2 \min(\nabla_i \nabla_j V) \leq -c'V$, where c and c' are positive order-one numbers [24,28]. Note that the constraint above precludes dS vacua where $\nabla V = 0$, and therefore rules out ΛCDM, even when $c \ll 1$ [42].

Studies of dynamical dark energy models that alleviate the H_0 tension have been carried out independently of the validity of the swampland conjectures [43,44]. One interesting type of models in this category deals with the scalar field playing the role of early dark energy, viz. the field could behave like a cosmological constant at early times (redshifts $z \gtrsim 3000$) and then dilute away like radiation or faster at later times [45–48]. If this were the case, the sound horizon at decoupling would be reduced resulting in a larger H_0 value inferred from BAO and CMB data. However, the CMB-preferred value of σ_8 (the rms density fluctuations within a top-hat radius of $8h_0^{-1}$ Mpc, with h_0 the dimensionless Hubble constant) increases in early dark energy models as compared to ΛCDM, increasing the tension with large-scale structure (LSS) data. More concretely, it is the combination $S_8 = \sigma_8(\Omega_m/0.3)^{0.5}$ that is constrained by LSS data, where Ω_m is the matter density. The Planck Collaboration reported $S_8 = 0.830 \pm 0.013$ [10] whereas local measurements find the smaller values; namely, $S_8^{\rm SZ} = \sigma_8(\Omega_m/0.27)^{0.3} = 0.78 \pm 0.01$ from Sunyaev-Zeldovich cluster counts [49], $S_8 = 0.773^{+0.026}_{-0.020}$ from DES [50] and $S_8 = 0.745 \pm 0.039$ from KiDS-450 [51] weak-lensing-surveys. The physical origin for the increase of σ_8 in early dark energy models is fairly straightforward, because the new dark-energylike component acts to slightly suppress the growth of perturbations during the period in which it contributes non-negligibly to the cosmic energy density. Henceforth, if we want to preserve the fit to the CMB data we must increase the CDM component to compensate for the suppression in the efficiency of perturbation growth [52].

A second type of interesting models emerges if dark energy and dark matter interact with each other [53–62]. The identification of the infinite tower of string states (following the swampland distance conjecture) as inhabiting the dark sector automatically provides a string framework for a concomitant coupling of the scalar field to the dark matter [63,64]. Within this framework there is a continually reduction of the dark matter mass as the scalar field rolls in the recent cosmological epoch. Such a reduction of the dark matter mass is actually compensated by a bigger value of dark energy density, which becomes visible in the present accelerating epoch calling for an increase of H_0. In this paper we present a well motivated realization of the cosmological string framework put forward by Agrawal, Obied, and Vafa (AOV) [63]. A point worth noting at this juncture is that the AOV models do not fully resolve the tension in H_0 measurements, as they can raise the ΛCDM predicted value of the Hubble constant only up to $H_0 = 69.06^{+0.66}_{-0.73}\ \mathrm{km\,s^{-1}\,Mpc^{-1}}$ [63]. Indeed, this maximum value of H_0 is characteristic of all models with late dark energy modification of the ΛCDM expansion history. This is because the local distance ladder calibrates SNe far into the Hubble flow and if dark matter fading takes place too recently then it would raise H_0 but without actually changing the part of the Hubble diagram where the tension is inferred. More concretely, by substituting the SH0ES calibration to the Pantheon SNe dataset, the ability of late times dark energy transitions to reduce the Hubble tension drops effectively to $H_0 = 69.17 \pm 1.09\ \mathrm{km\,s^{-1}\,Mpc^{-1}}$ [65]. However, the AOV proposal provides a novel cosmological set up that improves the fit to data compared to ΛCDM, while satisfying the dS swampland conjecture. Moreover, the smaller content of CDM at late times in AOV models as compared to ΛCDM yield a slight decrease of S_8, which can help reduce somewhat the tension between the CMB and LSS datasets.

Our starting point is Salam-Sezgin 6-dimensional supergravity (SUGRA) model, where a supersymmetric solution of the form $\mathrm{Minkowski}_4 \times S^2$ is known to exist, with a $U(1)$ monopole serving as background in the two-sphere [66]. This model can be lifted to string (and M) theory [67] and is asymptotic at large distances to the near-horizon limit of NS5-branes described by the linear dilaton background which is an exact string solution [68]. Moreover, the cosmological content of this supergravity model provides a solution of the field equations that can accommodate both the observed dark energy density and a fraction of CDM [69]. (Time dependence in the moduli fields vitiates invariance under supersymmetry transformations.) The carrier of the acceleration in the present dS epoch is a quintessence field slowly rolling down its exponential potential. Intrinsic to this

model is a second modulus, which is automatically stabilized and acts as a source of CDM, with a mass proportional to an exponential function of the quintessence field. The exponential functional form of the mass spectrum characterizes the infinite tower of mass states (inherent to the swampland distance conjecture), which emerges when the quintessence field moves a distance in field space $\gtrsim\mathcal{O}(1)$ in Planck units.

In the proposed cosmological framework, the standard model (SM) fields are confined to a probe brane and arise from quantum fluctuations. On the other hand, by computing the quantum fluctuations of the $U(1)$ field associated to the background configuration it is easily seen that the Kalb-Ramond field generates a mass term of horizon size [69]. These "paraphotons" (denoted herein by Υ) have been redshifting down since the quantum gravity era without being subject to reheating. The presence of any additional relativistic particle species with g degrees of freedom is usually characterized by

$$\Delta N_{\rm eff} \equiv N_{\rm eff} - N_{\rm eff}^{\rm SM} = g\left(\frac{10.75}{g_*(T_{\rm dec})}\right)^{4/3} \times \begin{cases} 4/7 & \text{boson} \\ 1/2 & \text{fermion} \end{cases}, \tag{1}$$

where $N_{\rm eff}$ quantifies the total relativistic "dark" energy density (including the three left-handed SM neutrinos) in units of the density of a single Weyl neutrino species [70] and $N_{\rm eff}^{\rm SM} = 3.046$ [71], and where $T_{\rm dec}$ is the temperature at which particle species decouple from the primordial plasma and the function $g_*(T_{\rm dec})$ is the number of effective degrees of freedom (defined as the number of independent states with an additional factor of $7/8$ for fermions) of the SM particle content at the temperature $T_{\rm dec}$. Comparing the 106.75 degrees of freedom of the SM with the 10.75 degrees of freedom of the primordial plasma before neutrino decoupling it is straightforward to see that for a massless (real) spin-0 scalar, spin-$\frac{1}{2}$ (Weyl) fermion, and massive spin-1 vector boson the contributions to $N_{\rm eff}$ asymptote to specific values of $\Delta N_{\rm eff} = 0.027$, 0.047, and 0.080; respectively [72].[1] Hence, fluctuations in the Kalb-Ramond field do not influence the primordial abundances of the nuclides produced at big-bang nucleosynthesis (BBN) as the Υ's only count for $\Delta N_{\rm eff} \lesssim 0.080$ and the 95% CL limit from a combination of current CMB, BAO, and BBN observations is $\Delta N_{\rm eff} < 0.214$ [10].[2]

The layout of the paper is as follows. In Sec. II we briefly describe the geometrical properties of unified dS-Friedmann models when embedded into Salam-Sezgin 6-dimensional supergravity. In Sec. III we interpret numerical results from data analysis that feature estimates for each free parameter in the model. We show that the Salam-Sezgin cosmological set up has the salient features of the generic Agrawal-Obied-Vafa model, and ergo can potentially ameliorate the tension between local distance ladder and cosmic microwave background estimates of H_0. In Sec. IV we comment on a viable solution to overcome the tension between low- and high-redshift observations within the AOV background. The paper wraps up with discussion and conclusions presented in Sec. V. Before proceeding, we note that other ideas relating cosmological observations to the swampland conjectures have been presented in [79–95].

II. EMBEDDING OF dS-FRIEDMANN MODEL INTO SALAM-SEZGIN SUGRA

Concentrating on the purely bosonic field content of Salam-Sezgin 6-dimensional SUGRA, we can express the bulk action of the system by

$$S \supset \frac{1}{4\kappa^2}\int d^6x\sqrt{g_6}\Big[R_6 - \kappa^2(\partial_M\sigma)^2 - \kappa^2 e^{\kappa\sigma}F_{MN}^2 - \frac{2g^2}{\kappa^2}e^{-\kappa\sigma} - \frac{\kappa^2}{3}e^{2\kappa\sigma}G_{MNP}^2\Big], \tag{2}$$

where $g_6 = \det g_{MN}$, R_6 is the Ricci scalar of g_{MN}, σ is a scalar field, $F_{MN} = \partial_{[M}A_{N]}$, $G_{MNP} = \partial_{[M}B_{NP]} + \kappa A_{[M}F_{NP]}$, A_N is a gauge field, B_{NP} is the Kalb-Ramond field, g is the $U(1)$ coupling constant, κ the gravitational coupling constant, and capital Latin indices run from 0 to 5 [66]. With redefinition of constants $G_6 \equiv 2\kappa^2$ and $\xi \equiv 4g^2$, and rescaling of $\phi \equiv -\kappa\sigma$ the action (2) takes the form

$$S \supset \frac{1}{2G_6}\int d^6x\sqrt{g_6}\Big[R_6 - (\partial_M\phi)^2 - \frac{\xi}{G_6}e^{\phi} - \frac{G_6}{2}e^{-\phi}F_{MN}^2 - \frac{G_6}{6}e^{-2\phi}G_{MNP}^2\Big], \tag{3}$$

where the length dimensions of the fields are $[G_6] = L^4$, $[\xi] = L^2$, $[\phi] = [g_{MN}^2] = 1$, $[A_M^2] = L^{-4}$, and $[F_{MN}^2] = [G_{MNP}^2] = L^{-6}$.

Note that by rescaling the 6-dimensional metric as $g_{MN} \to e^{-\phi}g_{MN}$, one finds the action at the string frame where ϕ-dependence enters as an overall exponential factor $e^{-2\phi}$. ϕ is then identified with the string dilaton, defining the string coupling e^{ϕ} and having a tree-level potential corresponding to a noncritical string with the parameter ξ determined by the central charge deficit. The latter is induced by the compactification of the four internal dimensions on a manifold with nonvanishing curvature. Its sign implies that the internal curvature is negative, such as the noncompact $H^{(2,2)} \times S^1$ space considered in [67] to

[1] Asymptote here refers to relativistic species decoupling just before top quark freeze-out.

[2] This limit combines the helium measurements of [73,74] with the latest deuterium abundance measurements of [75] using the PARTHENOPE code [76] considering $d(p,\gamma)^3$He reaction rates from [77]. Should one instead use the helium abundance measurement of [78] in place of [73,74], the 95% CL limit on the equivalent neutrino species shifts, $N_{\rm eff} = 3.37 \pm 0.22$, and is in 2.9σ tension with the SM value.

compactify from 10 to 6 dimensions. Its compact analytic continuation is $S^3 \times S^1$, which has an exact (super)-conformal field theory description, since S^3 corresponds to an $SU(2)_k$ Wess-Zumino-Witten model with curvature fixed by the level k. The total internal 6-dimensional space of our model is then $H^{(2,2)} \times S^1 \times S^2$, with the monopole field on S^2. The exponential dilaton potential does not allow for static solutions. One solution is the linear dilaton background along a space direction which has an exact string description in terms of a free coordinate with background charge. It corresponds to the near horizon limit of NS5-branes which is holographic dual to a little string theory [96]. In our case of interest, ξ is positive and the solution becomes linear dilaton in the time coordinate with flat metric in the string frame (σ-model) [68]. In the Einstein frame, the scale factor of the metric in FRW coordinates grows linearly with time while the dilaton dependence becomes logarithmic. This exact time dependent "vacuum" solution is the only asymptotic at large times, even in the presence of matter, as we will see later.

We can now carry out a spontaneous compactification from six to four dimensions, considering the 6-dimensional manifold M of the base spacetime to be a direct product of 4 Minkowski directions (hereafter denoted by M_4) and the 2-sphere, $\mathbb{R}^{1,3} \times S^2$. The line element on M locally is given by

$$ds_6^2 = ds_4(t,\vec{x})^2 + e^{2f(t,\vec{x})} r_c^2 (d\vartheta^2 + \sin^2\vartheta d\varphi^2), \quad (4)$$

where $(t,\vec{x})$ denotes a local coordinate system in M_4, r_c is the compactification radius, and f is the breathing mode of the compact space. We assume that the scalar field ϕ depends only on the point of M_4, i.e., $\phi = \phi(t,\vec{x})$. We further assume that the gauge field A_M is excited on S^2 and is of the form

$$A_\vartheta = 0 \quad \text{and} \quad A_\varphi = b\cos\vartheta; \quad (5)$$

this is the monopole configuration detailed in [66]. For the purpose of this work, we will set the Kalb-Ramond field to its zero background value, $B_{NP} = 0$, and since the term $A_{[M}F_{NP]}$ vanishes on S^2, we have $G_{MNP} = 0$. The field strength becomes

$$F_{MN}^2 = 2b^2 e^{-4f}/r_c^4. \quad (6)$$

Taking the variation of the gauge field A_M in (3) we obtain the Maxwell equation

$$\partial_M[\sqrt{g_4}\sqrt{g_\sigma} e^{2f-\phi} F^{MN}] = 0. \quad (7)$$

It is straightforward to verify that the field strength in (6) satisfies (7).

Without loss of generality, the Ricci scalar can be written as

$$R_6 \equiv R[M] = R[M_4] + e^{-2f} R[S^2] - 4\Box f - 6(\partial_\mu f)^2, \quad (8)$$

where $R[M]$, $R[M_4]$, and $R[S^2] = 2/r_c^2$ denote respectively the Ricci scalars of the manifolds M, M_4 and S^2, with Greek indices running from 0 to 3 [97]. To simplify the notation hereafter R_4 and R_2 indicate $R[M_4]$ and $R[S^2]$, respectively. The determinant of the metric can be written as $\sqrt{g_6} = e^{2f}\sqrt{g_4}\sqrt{g_2}$, where $g_4 = \det g_{\mu\nu}$ and $g_2 = r_c^4 \sin^2\vartheta$ is the determinant of the metric of S^2 excluding the factor e^{2f}. We define the gravitational constant in the four dimension as

$$\frac{1}{G_4} \equiv \frac{M_{\rm Pl}^2}{2} = \frac{1}{2G_6}\int \sqrt{g_2}(d\vartheta \wedge d\varphi) = \frac{2\pi r_c^2}{G_6}. \quad (9)$$

Thus and so, by using the field configuration given in (5) the action in (3) can be recast as

$$S \supset \frac{1}{G_4}\int d^4x\sqrt{g_4}\Big\{ e^{2f}[R_4 + e^{-2f}R_2 + 2(\partial_\mu f)^2 - (\partial_\mu\phi)^2] - \frac{\xi}{G_6}e^{2f+\phi} - \frac{G_6 b^2}{r_c^4}e^{-2f-\phi} - \frac{G_6}{2}e^{2f-\phi}F_{\mu\nu}^2\Big\}, \quad (10)$$

where we included the last term that does vanish identically to show what is the 4-dimensional coupling of gauge fields that come from 6 dimensions in the Neveu-Schwarz (NS) sector. In the spirit of [42], we now consider a rescaling of the metric of M_4 such that $\hat{g}_{\mu\nu} \equiv e^{2f} g_{\mu\nu}$ and therefore $\sqrt{\hat{g}_4} = e^{4f}\sqrt{g_4}$. The preceding metric transformation brings the model into the Einstein frame, in which the action given in (10) can be rewritten as

$$S \supset \frac{1}{G_4}\int d^4x\sqrt{\hat{g}_4}\Big[R[\hat{g}_4] - 4(\partial_\mu f)^2 - (\partial_\mu\phi)^2 - \frac{\xi}{G_6}e^{-2f+\phi} - \frac{G_6 b^2}{r_c^4}e^{-6f-\phi} + e^{-4f}R_2 - \frac{G_6}{2}e^{2f-\phi}F_{\mu\nu}^2\Big], \quad (11)$$

and we can use $\hat{g}_4$ in this frame to define a metric which we use to measure distances in the field space. The effective Lagrangian density in 4 dimensions takes the form

$$\mathcal{L} \supset \frac{\sqrt{g}}{G_4}[R - 4(\partial_\mu f)^2 - (\partial_\mu\phi)^2 - V(f,\phi)], \quad (12)$$

with

$$V(f,\phi) \equiv \frac{\xi}{G_6}e^{-2f+\phi} + \frac{G_6 b^2}{r_c^4}e^{-6f-\phi} - e^{-4f}R_2, \quad (13)$$

where to simplify the notation we have defined: $g \equiv \hat{g}_4$ and $R \equiv R[\hat{g}_4]$.

Next, we define a new orthogonal basis, $X \equiv (\phi + 2f)/\sqrt{G_4}$ and $Y \equiv (\phi - 2f)/\sqrt{G_4}$, so that the kinetic energy terms in the Lagrangian are both canonical, i.e.,

$$\mathcal{L} \supset \sqrt{g}\left[\frac{R}{G_4} - \frac{1}{2}(\partial X)^2 - \frac{1}{2}(\partial Y)^2 - \tilde{V}(X,Y)\right], \quad (14)$$

where the potential $\tilde{V}(X,Y) \equiv V(f,\phi)/G_4$ can be rewritten (after some elementary algebra) as [98]

$$\tilde{V}(X,Y) = \frac{e^{\sqrt{G_4}Y}}{G_4}\left[\frac{G_6 b^2}{r_c^4}e^{-2\sqrt{G_4}X} - R_2 e^{-\sqrt{G_4}X} + \frac{\xi}{G_6}\right]. \quad (15)$$

Note that Y corresponds to the 4-dimensional dilaton. The equations of motion for the X and Y fields are

$$\Box X = \partial_X \tilde{V} \quad \text{and} \quad \Box Y = \partial_Y \tilde{V}, \quad (16)$$

and the Einstein field equations are

$$R_{\mu\nu} - \frac{1}{2}g_{\mu\nu}R = \frac{G_4}{2}\left[\left(\partial_\mu X \partial_\nu X - \frac{g_{\mu\nu}}{2}\partial_\eta X \partial^\eta X\right) + \left(\partial_\mu Y \partial_\nu Y - \frac{g_{\mu\nu}}{2}\partial_\eta Y \partial^\eta Y\right) - g_{\mu\nu}\tilde{V}(X,Y)\right] + T'_{\mu\nu}, \quad (17)$$

where we have added the matter and radiation stress-energy tensor $T'_{\mu\nu}$, which also contributes to the evolution of the Universe. To allow for a dS era we assume that the metric takes the form

$$ds^2 = -dt^2 + e^{2h(t)}d\vec{x}^2, \quad (18)$$

and that X and Y depend only on the time coordinate, i.e., $X = X(t)$ and $Y = Y(t)$.

Before proceeding, we pause to present our notation. Throughout, the subindex zero indicates quantities which are evaluated today. As usual, we normalize the Hubble parameter to its value today introducing an adimensional parameter $H_0 = 100h_0\ \mathrm{km\,s^{-1}\,Mpc^{-1}}$. Note that the function $h(t)$ in the metric measures the evolution of H, with $h(t_0) = h_0$. Now, we can rewrite (16) as

$$\ddot{X} + 3\dot{h}\dot{X} = -\partial_X \tilde{V} \quad \text{and} \quad \ddot{Y} + 3\dot{h}\dot{Y} = -\partial_Y \tilde{V}, \quad (19)$$

and the nonzero independent components of (17) are

$$\dot{h}^2 = \frac{G_4}{6}\left[\frac{1}{2}(\dot{X}^2 + \dot{Y}^2) + \tilde{V}(X,Y)\right] + \frac{\rho'}{3} \quad (20)$$

and

$$2\ddot{h} + 3\dot{h}^2 = \frac{G_4}{2}\left[-\frac{1}{2}(\dot{X}^2 + \dot{Y}^2) + \tilde{V}(X,Y)\right] - p', \quad (21)$$

where p and ρ' are the pressure and energy density contained in $T'_{\mu\nu}$.

The terms in the square brackets in (15) take the form of a quadratic function of $e^{-\sqrt{G_4}X}$. This function has a global minimum at $e^{-\sqrt{G_4}X_0} = R_2 r_c^4/(2G_6 b^2)$, and so we expand (15) around the minimum,

$$\tilde{V}(X,Y) = \frac{e^{\sqrt{G_4}Y}}{G_4}\left[\mathcal{K} + \frac{\overline{M_X}^2}{2}(X - X_0)^2 + \mathcal{O}((X - X_0)^3)\right], \quad (22)$$

where

$$\overline{M_X} \equiv \frac{1}{\sqrt{\pi}\, b r_c} \quad (23)$$

and

$$\mathcal{K} \equiv \frac{M_{\mathrm{Pl}}^2}{4\pi r_c^2 b^2}(b^2\xi - 1). \quad (24)$$

Obviously the scalar field X is stabilized around its minimum X_0. Its physical mass is Y-dependent,

$$M_X(Y) = \frac{e^{\sqrt{G_4}Y/2}}{\sqrt{G_4}}\overline{M_X}, \quad (25)$$

and characterizes the mass scale of the tower of string states, which according to the infinite distance conjecture becomes exponentially massless [20,21,28,37–39]. Indeed, as Y runs to large and negative values the 4-dimensional Planck mass grows exponentially as $M_{\mathrm{Pl}} \sim e^{-Y}$ in string units, and thus string excitations become exponentially light in Planck units. Note though that these states cannot play the role of dark matter since part of the string modes carry also SM gauge charges. The X particle on the other hand can play the role of fading dark matter, as we show in the next section.

In the absence of matter and radiation described by the stress tensor $T'_{\mu\nu}$, the equations of motion (19)–(21) have no dS or inflationary solution. As we mentioned above, there is an exact string solution with both functions h and Y logarithmic in time describing a linearly expanding universe, which corresponds in the string frame to the well know linear dilaton and flat metric background. This requires the parameter $\mathcal{K}$ in Eq. (22) to be positive. As we will see later, this solution becomes asymptotic at large times in the presence of matter and radiation. Moreover, there is a period in time of approximate exponential expansion. The dS (vacuum) potential energy density is given by

$$V_Y = \frac{e^{\sqrt{G_4}Y}}{G_4}\mathcal{K}. \quad (26)$$

Now, the requirements for preserving a fraction of supersymmetry (SUSY) in spherical compactifications to four

dimension imply $b^2\xi = 1$, corresponding to winding number $n = \pm 1$ for the monopole configuration [66]. From (24) and (26) it follows that the condition for the potential to show a dS rather than an AdS or Minkowski phase is $\xi b^2 > 1$. Therefore, we conclude that a (Y-dependent) dS background can be obtained only through SUSY breaking; see Appendix for details.

We finish this section with a comment on possible SM embeddings. In principle, excitations of the electromagnetic field would seemingly induce variation in the electromagnetic fine structure constant, as well as a violation of the equivalence principle through a long range coupling of the dilaton to the electromagnetic component of the stress tensor [99]. A similar variation would be induced in the QCD gauge coupling and thus in the hadron masses. Although a preliminary analysis seems to indicate that such variations may still be compatible with experimental limits because the resulting range of variation of the quintessence field is about 2.5 Planck units (see next section), a very light dilaton would also mediate extra forces at short and larger distances [100] which are excluded in particular by microgravity experiments [101]. A possible way out would be to confine the SM fields on NS5-branes [102]. The 6-dimensional gauge couplings are then independent of the string dilaton in the string frame and thus come with a factor e^{ϕ} instead of $e^{-\phi}$ in the Einstein frame, see Eq. (3). It follows that upon compactification to four dimensions, gauge kinetic terms couple to $e^{2f+\phi}$, see Eq. (11), and thus the 4-dimensional gauge couplings depend on the scalar X (instead of the dilaton Y) which is fixed at the minimum of the potential, and SM couplings do not vary. Moreover, one avoids direct couplings of the dilaton to matter suppressing extra forces competing with gravity.

III. REDUCING THE H_0 TENSION WITH FADING DARK MATTER

We now turn to investigate the cosmological implications of the Salam-Sezgin model, by accommodating recent cosmological observations, while seeking to diminish the tension between low- and high-redshift measurements. To do so, we adopt the best fit value of $H_0 = 69.06^{+0.66}_{-0.73}\ \mathrm{km\,s^{-1}\,Mpc^{-1}}$ in the AOV study [63] and analyze the dependence of the quantities relevant to cosmology on the model parameters.

The total energy density of the Universe, $\rho = \sum_i \rho_i$, drives the evolution of the Hubble parameter H, where $i = \{X, Y, \mathcal{X}, b, r\}$ accounts for the X and Y fields, for other types of dark matter $\mathcal{X}$, and for the usual SM components of baryonic matter b and radiation r. For a spatially flat Universe, $H^2 = \rho/3$, where we have adopted reduced Planck units, i.e., $M_{\rm Pl} = 1$ and $G_4 = \sqrt{2}$. For convenience, herein we consider the evolution in $u \equiv -\ln(1+z)$ rather than t, where z is the redshift parameter. With this in mind, we express the evolution of the matter and radiation components as

$$\rho_b = \rho_{b,0} e^{-3u}, \tag{27a}$$

$$\rho_{\mathcal{X}} = \rho_{\mathcal{X},0} e^{-3u}, \tag{27b}$$

and

$$\rho_r = \rho_{r,0} e^{-4u} f(u), \tag{27c}$$

where we remind the reader that the subindex zero indicates quantities which are evaluated today, and $f(u)$ parametrizes the u dependent number of radiation degrees of freedom. For the sake of interpolating the various thresholds appearing prior to recombination (among others, QCD and electroweak), we adopt a convenient phenomenological form derived elsewhere $f(u) = e^{-u/15}$ [103]. To simplify notation we also conveniently define $\rho_* = \rho_b + \rho_{\mathcal{X}}$. A point worth noting at this juncture is that the leading term in the expansion of the potential $\tilde{V}$ around the local minimum X_0 is quadratic, and therefore the coherent X-field energy behaves like nonrelativistic dark matter [104]. Thus, the X pressureless dark matter and $\mathcal{X}$ add up to the CDM of our model. All in all, the number density of the field X evolves like that of a matter term (i.e., proportional to e^{-3u}), while its mass evolves with Y according to (25). Therefore, as in the AOV scheme [63], we have

$$\begin{aligned}\rho_X = M_X n_X &= \rho_{X,0} \exp\left(\frac{Y - Y_0}{\sqrt{2}} - 3u\right) \\ &= A \exp\left(\frac{Y}{\sqrt{2}} - 3u\right).\end{aligned} \tag{28}$$

Finally, the energy density for Y is found to be

$$\rho_Y = \frac{1}{2} H^2 Y'^2 + V_Y. \tag{29}$$

Now, making use of the preceding formulas, we can give an explicit expression for the evolution of the Hubble parameter:

$$H^2 = \frac{\rho_{\rm s}}{3 - Y'^2/2}, \tag{30}$$

where $\rho_{\rm s} = \rho_* + \rho_r + V_{\rm eff}$ stands for the *steady-state* energy density in moduli space, in the sense that the field Y is not evolving ($Y' = 0$), with $V_{\rm eff} \equiv V_Y + \rho_X$. These definitions allow us to rewrite the evolution equation (19) for Y as

$$\frac{Y''}{1 - \frac{1}{6}Y'^2} + 3Y' + \frac{\frac{1}{2}Y'\partial_u \rho_{\rm s} + 3\partial_Y V_{\rm eff}}{\rho_{\rm s}} = 0. \tag{31}$$

Next, to simplify the numerical solution to the last equation, we introduce the parameters

$$\alpha \equiv \frac{V_0}{\rho_{*,0}}, \tag{32a}$$

$$\beta \equiv \frac{\rho_{r,0}}{\rho_{*,0}}, \tag{32b}$$

and

$$\gamma \equiv \frac{A}{\rho_{*,0}}, \tag{32c}$$

where $V_0 \equiv V_Y|_{Y=0} = \mathcal{K}/\sqrt{2}$. Further definition of $\rho_s \equiv \rho_{*,0}\bar{\rho}_s$ and $V_{\rm eff} \equiv \rho_{*,0}\bar{V}_{\rm eff}$, which depend only on the parameters introduced in (32), makes explicit the dependence of the solution to (31) on just α, β, and γ. Following [69], we take as initial conditions $Y(-30) = 0$ and $Y'(-30) = 0.08$, which are in accordance to equipartition arguments [105,106].

In order to understand to which extent this model can represent cosmological data, we introduce the density parameters $\Omega_i = \rho_i/3H^2$ and the equation of state for the field Y:

$$w_Y \equiv \frac{p_Y}{\rho_Y} = \frac{\frac{1}{2}H^2Y'^2 - V_Y}{\frac{1}{2}H^2Y'^2 + V_Y}. \tag{33}$$

At this stage, it is worthwhile to note that although the solution for Y only depends on α, β and γ, the cosmological quantities depend on additional parameters. For instance, the use of (30) and (33) requires the introduction of $\rho_{m,0} = \rho_{*,0} + \rho_{X,0}$ and h_0 as additional parameters. This amounts to a total of five free parameters in this model. For future convenience, they are chosen to be h_0, $\Omega_{m,0}$, $\Omega_{r,0}$, $a \equiv A/(3H_0^2)$ and $v_0 \equiv V_0/(3H_0^2)$. These parameters are constrained by five conditions. One is the use of (30) as an internal consistency condition on the total energy density. Four additional constraints will come as an attempt to reproduce experimental data with this model. In particular, we will fix h_0 to an experimental value $\tilde{h}_0$, and subsequently fixing the radiation content of the universe, since this model does not provide any mechanism to modify it, with the additional constraint

$$\Omega_{r,0} = \tilde{\Omega}_{r,0} \equiv \frac{\Omega_{r,0}h_0^2|_{\rm exp}}{\tilde{h}_0{}^2}. \tag{34}$$

The total matter content of our model is similarly adjusted to an experimental value and is given by

$$\Omega_{m,0} \equiv \Omega_{*,0} + \Omega_{X,0} = \tilde{\Omega}_{m,0} = \frac{\Omega_{m,0}h_0^2|_{\rm exp}}{\tilde{h}_0^2}. \tag{35}$$

Before we go any further, we clarify that a tilde on top of a given parameter of the model, identifies its direct experimental measurement, and when the measured quantity is a product of two model parameters then we adopt the subindex exp to indicate the experimental measurement. Finally, the equation of state for Y today is fixed to the value of the dark energy equation of state $w_{Y,0} = \tilde{w}_{Y,0}$. In our calculations we take $\tilde{w}_{Y,0} = -0.80^{+0.09}_{-0.11}$, as derived from a combination of multiple observational probes in the Dark Energy Survey (DES) supernovae program (including 207 type Ia supernovae light curves, the BAO feature, weak gravitational lensing, and galaxy clustered, but independent of CMB measurements) [107]. This value of $\tilde{w}_{Y,0}$ is consistent at the 1σ level with the one derived from a combination of DES data and CMB measurements [108].

Making use of (33) and (32a), we can rewrite the constraint on the equation of state as

$$\tilde{w}_{Y,0} = \frac{\frac{1}{6}Y_0'^2 - v_0e^{\sqrt{2}Y_0}}{\frac{1}{6}Y_0'^2 + v_0e^{\sqrt{2}Y_0}}. \tag{36}$$

Making use of (30) at $u = 0$ together with (34) and (35) we arrive at

$$\frac{1}{6}Y_0'^2 = 1 - \tilde{\Omega}_{r,0} - \tilde{\Omega}_{m,0} - v_0e^{\sqrt{2}Y_0}, \tag{37}$$

which can be substituted into (36) to find the constraint

$$v_0e^{\sqrt{2}Y_0} = c_-. \tag{38}$$

Moreover, this result can be substituted back into (37) to find a second constraint: $Y_0'^2 = 6c_+$. We have defined the experimentally determined constants

$$c_\pm \equiv \frac{1 \pm \tilde{w}_{Y,0}}{2}(1 - \tilde{\Omega}_{m,0} - \tilde{\Omega}_{r,0}). \tag{39}$$

The third independent constraint between the still free parameters $\Omega_{*,0}$, a, and v_0 can be found as a result of (38) and $\Omega_{X,0} = ae^{Y_0/\sqrt{2}}$, and is given by

$$v_0 = c_-\left(\frac{a}{\tilde{\Omega}_{m,0} - \Omega_{*,0}}\right)^2 = c_-\left(\frac{a}{\Omega_{X,0}}\right)^2, \tag{40}$$

unless $a = \Omega_{X,0} = 0$. Under this condition, v_0 can be determined from a and $\Omega_{X,0}$, in which case the full solution comes from the solution to the system

$$Y_0 = \sqrt{2}\ln\left(\frac{\Omega_{X,0}}{a}\right), \tag{41a}$$

$$Y_0'^2 = 6c_+. \tag{41b}$$

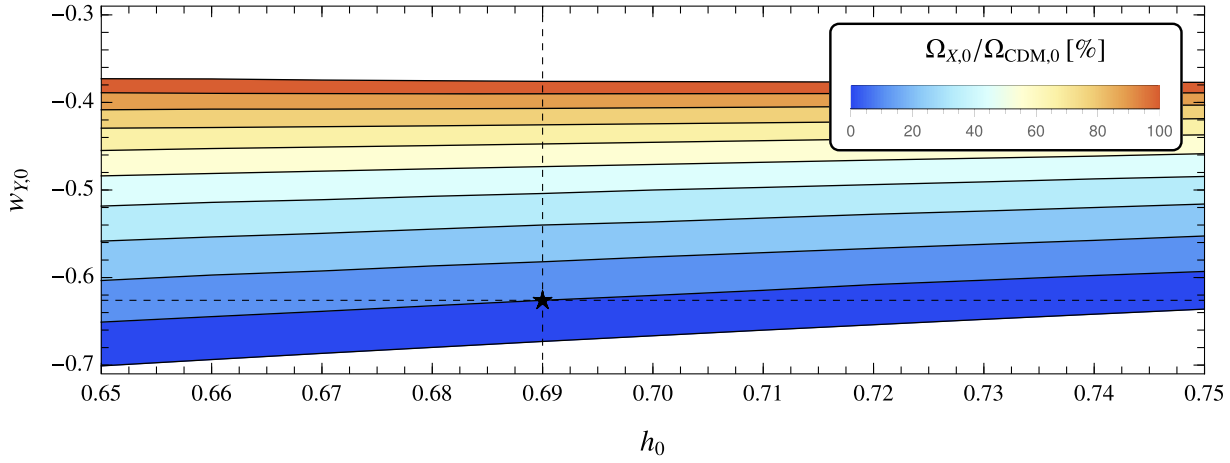

FIG. 1. Allowed region in the $(h_0, w_{Y,0})$ parameter space, in terms of the ratio of present energy densities for the X-field and the total CDM. The star indicates the preferred h_0 value in the AOV analysis [63].

It must be noted that both Y_0 and ${Y'_0}^2$ are functions of $\Omega_{X,0}$ and a through their dependence on the parameters α, β and γ from (32). Solving separately (41a) and (41b) we can obtain two solutions $\Omega^{(1)}_{X,0}(a)$ and $\Omega^{(2)}_{X,0}(a)$ respectively. A common solution exists if there is some a such that $\Omega^{(1)}_{X,0}(a) = \Omega^{(2)}_{X,0}(a)$. In the case that $a = \Omega_{X,0} = 0$ and $\Omega_{*,0} = \Omega_{m,0}$, the remaining parameter v_0 cannot be determined through (40), and its values $v_0^{(1)}$ and $v_0^{(2)}$ will come from the solutions to (38) and (41b), respectively, expressing Y_0 and Y'_0 as functions of v_0.

In the following we will consider the matter and radiation parameters as given by the Particle Data Group, $\Omega_{b,0}h_0^2|_{\mathrm{exp}} = 0.02226(23)$, $\Omega_{\mathrm{CDM},0}h_0^2|_{\mathrm{exp}} = 0.1186(20)$, and $\Omega_{r,0}h_0^2|_{\mathrm{exp}} = 2.473 \times 10^{-5}(T_{\gamma,0}/2.7255)^4$, where $T_{\gamma,0}$ is the temperature of the relic photons [109]. The existence of solutions to (41) is conditioned by the values of $\tilde{h}_0$ and $\tilde{w}_{Y,0}$ through the constants $c_\pm$. For example, for $(\tilde{h}_0, \tilde{w}_{Y,0}) = (0.71, -0.62)$, there exists a solution for $(\Omega_{X,0}, a) \approx (0.019, 0.107)$ but there is no solution for $(\tilde{h}_0, \tilde{w}_{Y,0}) = (0.71, -1)$. A systematic analysis of the $(\tilde{h}_0, \tilde{w}_{Y,0})$ parameter space is necessary to study the potential of this model.

For large values of a, it can be seen that $\Omega^{(2)}_{X,0}$ is consistently larger than $\Omega^{(1)}_{X,0}$, in a wide region of the $(\tilde{h}_0, \tilde{w}_{Y,0})$ parameter space. This can be used to study the existence of solutions. As $\Omega_{X,0}$ and a go to zero simultaneously, they do it as

$$\Omega_{X,0} = \sqrt{\frac{c_-}{v_0}}a, \tag{42}$$

as follows from (40). To ensure consistency with the solutions at $a = \Omega_{X,0} = 0$, each function $\Omega^{(i)}_{X,0}$ must have a different slope

$$\Omega^{(i)}_{X,0} = \sqrt{\frac{c_-}{v_0^{(i)}}}a. \tag{43}$$

Using this, if $v_0^{(2)} > v_0^{(1)}$, both curves must cross, guaranteeing the existence of a solution. The limiting condition $v_0^{(2)} = v_0^{(1)}$, which determines the existence of a solution with $a = 0$, separates both regions in the $(\tilde{h}_0, \tilde{w}_{Y,0})$ parameter space. In Fig. 1 we show this limiting condition together with several solutions for $a \neq 0$. The best fit value of [63], $h_0 = 0.69$, is indicated by a star. We note that models with $\Omega_{X,0}/\Omega_{\mathrm{CDM},0} \gtrsim 40\%$ are in 3σ tension with current determinations of $w_{Y,0}$.

We now take the best fit solution derived in [63] as the experimental value of H_0 and check for consistency of the relevant cosmological parameters. For $h_0 = 0.69$ and $\Omega_{X,0}/\Omega_{\mathrm{CDM},0} = 0.1$, we obtain $w_{Y,0} = -0.63$, which gives $a = 0.178$, $v_0 = 35.3$, and $V_0 = 3H_0^2 v_0 = 3.87 \times 10^{-119}$ in reduced Planck units.

The main results of the consistency investigation are encapsulated in Figs. 2–6, where we show the evolution of: (i) $Y(u)$ and $Y'(u)$, (ii) the various contributions to the total energy density, (iii) w_y, (iv) the acceleration parameter $-q(u) = 1 + h'(u)/h(u)$, and (v) the Hubble parameter. The results shown in the left panels of these figures are based on the best fit value of the AOV analysis (corresponding to $a = 0.178$), whereas those displayed in the right panels correspond to $a = 0$. For $a = 0$, we take $h_0 = 0.66$ and $w_{Y,0} = -0.70$; a choice justified below. We can see in Fig. 3 how the X-Y coupling depletes dark matter into dark energy, yielding a larger $\Omega_{Y,0} = 0.704$ for $a = 0.178$ than for $a = 0$ where $\Omega_{Y,0} = 0.673$. This is the so-called "fading dark matter" effect [63], which tends to favor larger values of h_0 when $a \neq 0$; namely, $h_0 = 0.69$ for $a = 0.178$, and $h_0 = 0.66$ for $a = 0$. The dark energy equation of state also shows striking differences. As we can see in the left panel Fig. 4, for $-10 \lesssim u \lesssim -2$. the dark

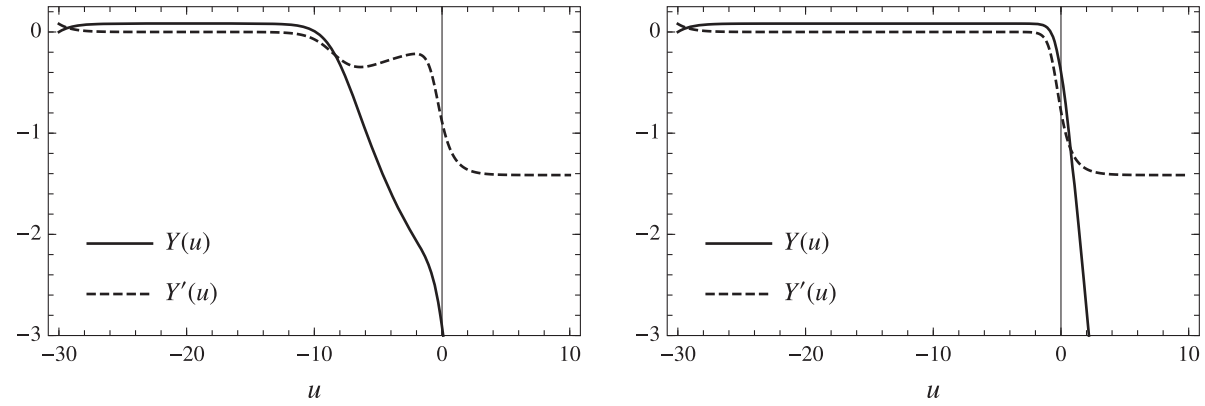

FIG. 2. Evolution of $Y(u)$ and $Y'(u)$, for $a = 0.178$ (left) and $a = 0$ (right).

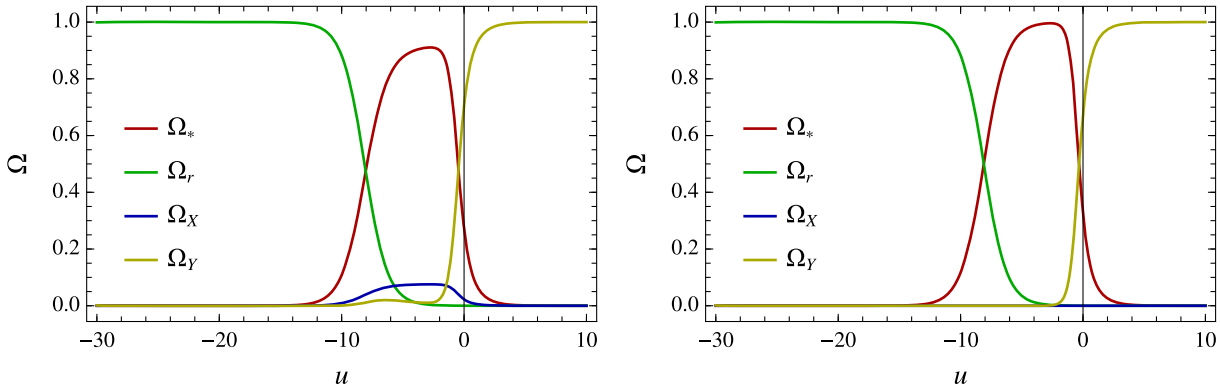

FIG. 3. Evolution of the density parameters Ω_r, Ω_*, Ω_X, and Ω_Y. We have taken $a = 0.178$ (left) and $a = 0$ (right).

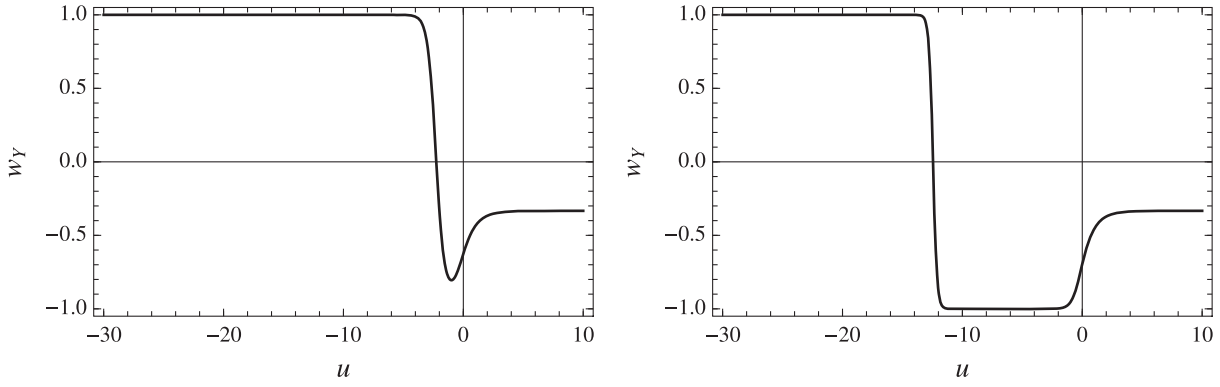

FIG. 4. Evolution of the equation-of-state parameter for dark energy w_Y, for $a = 0.178$ (left) and $a = 0$ (right).

energy equation of state $w_Y > 0$, so that the energy density redshifts faster than that in ΛCDM [63]. For $a = 0$, however, the dark energy equation of state mimics that of a cosmological constant, $w_Y = -1$, between $-10 \lesssim u \lesssim -2$. This translates into smaller values of $w_{Y,0}$ for the decoupled system with $a = 0$, and closer to the ΛCDM prediction of $w_\Lambda = -1$.

In the left panel of Fig. 7 we show 1, 3 and 5σ probability contours in the $(h_0, w_{Y,0})$ parameter space after performing a least squares fit of the model to the Hubble parameter data. The minimum, which corresponds to $a = 0$, corroborates that quintessence models exacerbate the H_0 tension since the dark energy density decreases in recent times [63]. As can be seen in the right panel of Fig. 7, the best fit value of h_0 in the OAV-study is consistent with determinations of $w_{Y,0}$ at $< 2\sigma$ level. We conclude that the set up introduced in Sec. II has the salient cosmological features of the AOV fading dark matter proposal.

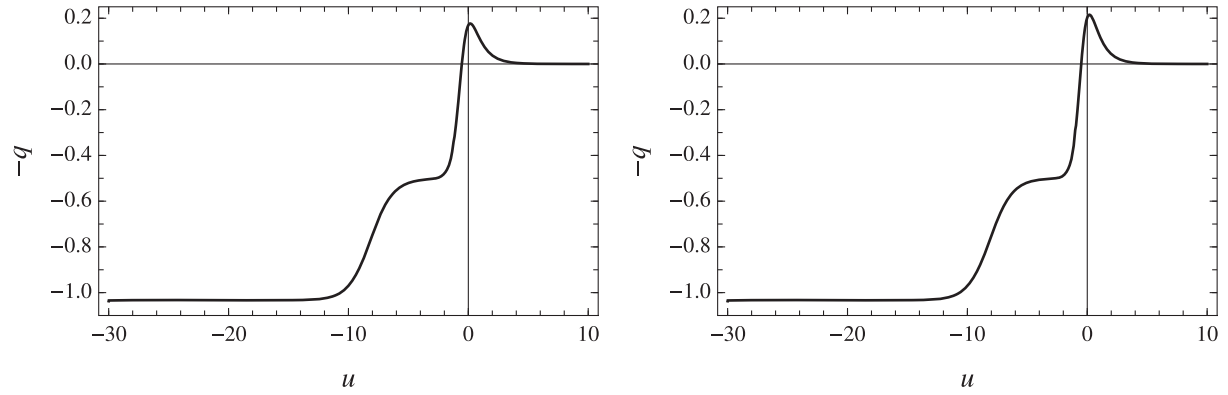

FIG. 5. Evolution of the acceleration parameter $-q$, for $a = 0.178$ (left) and $a = 0$ (right), showing the existence of an accelerated phase that asymptotically approaches a constant velocity expansion in the future.

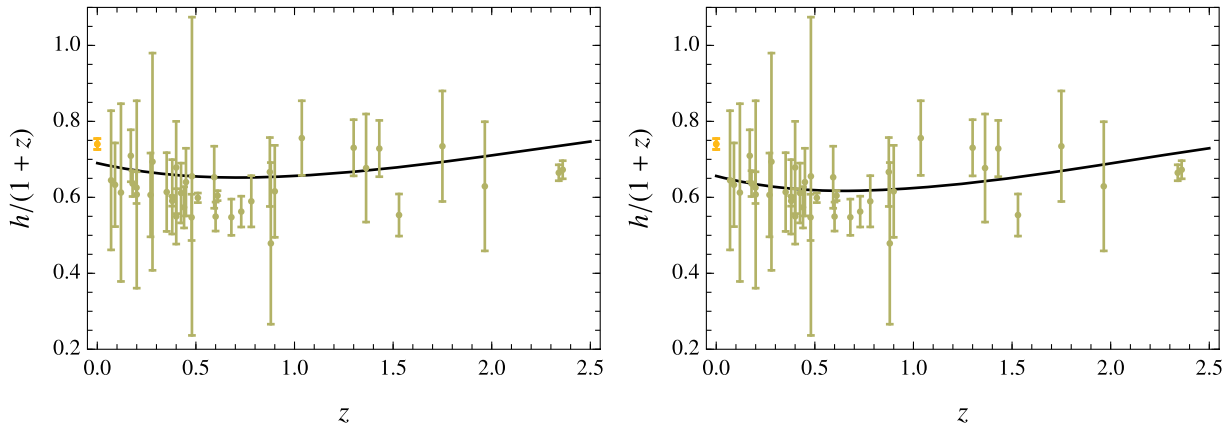

FIG. 6. Hubble expansion history for $z < 2.5$ considering $a = 0.178$ (left) and $a = 0$ (right). For comparison, we show the recent determination of h_0 from [7] together with a compilation [110] of 38 measurements $h(z)$ in the range $0 \leq z \leq 2.36$ [111–120]. These 38 $h(z)$ measurements are not completely independent. For example, the 3 measurements taken from [119] are correlated with each other, and the 3 measurements of [120] are correlated too. In addition, in these and other cases, when BAO observations are used to measure $h(z)$, one has to apply a prior on the radius of the sound horizon, $r_d = \int_{z_d}^{\infty} c_s(z)dz/H(z)$, evaluated at the drag epoch z_d, shortly after recombination, when photons and baryons decouple. This prior value of r_d is usually derived using CMB observations.

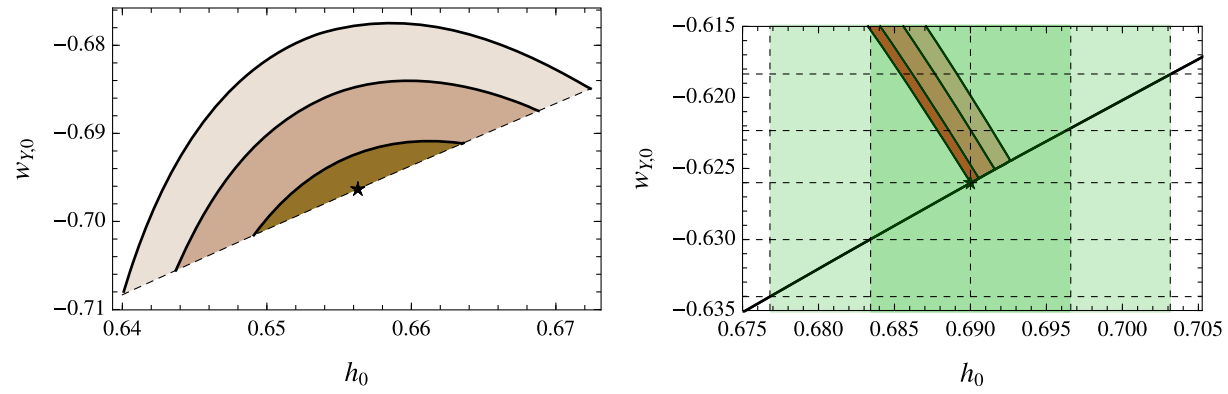

FIG. 7. Left panel. 1, 3 and 5σ probability contours in the $(h_0, w_{Y,0})$ parameter space after performing a least squares fit of the model to the Hubble parameter data. The minimum corresponds to $a = 0$. Right panel. Structure of the $(h_0, w_{Y,0})$ parameter space around the point $(h_0, w_{Y,0}) = (0.69, -0.626)$, indicated with a "⋆." The diagonal line separates the regions with $\Omega_{X,0}/\Omega_{\mathrm{CDM},0}$ larger (above) and smaller (below) than 0.1. The green bands indicate the 1 and 2σ confidence intervals for the value of h_0 as determined by SH0ES. The colored contours show constant χ^2 lines, after the fit shown in the left panel. The first from the left shows the values as likely as (0.69, −0.626), and the other three show the values such that $\Delta\chi^2$ is 1, 3 and 5, from left to right.

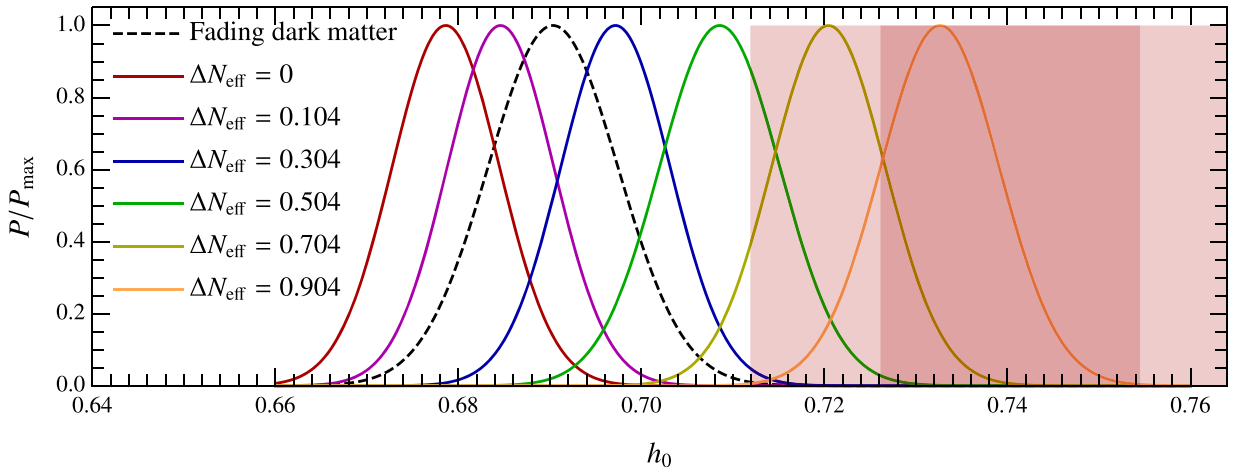

FIG. 8. Rescaled posterior distributions of h_0 (due to marginalization over additional free parameters) with different choices of $N_{\rm eff}$ from the 7 parameter fir of [130]. The rescaled posterior distribution of h_0 for the AOV fit is indicated with the dashed curve [63]. The shaded areas indicate the 1σ and 2σ regions as determined by SH0ES [7].

IV. HUBBLE HULLABALOO AND D-BRANE STRING COMPACTIFICATIONS

In this section we comment on additional phenomena that would influence the time evolution of the model parameters and may help solving the H_0 problem. It is common knowledge that D-brane string compactifications provide a collection of building block rules that can be used to build up the SM or something very close to it [121–123]. Gauge bosons of the brane stacks belong to $\mathcal{N} = 1$ vector multiplets together with the corresponding gauginos. At brane intersections chiral fermions belong to chiral multiplets denoted by their left-handed fermionic components Q, L, U^c, D^c, E^c, N^c, where the superscript c stands for the charged conjugate in the familiar notation.

For such D-brane constructs, superpotentials of the form MN^cN^c or SN^cN^c are precluded by the $U(1)_L$ lepton and $U(1)_{I_R}$ isospin-right gauge invariances, where M is a Majorana mass matrix in flavor space and S is a gauge singlet. Because of this, there is no equivalent to the seesaw mechanism to generate the Weinberg term [124] which gives rise to Majorana neutrinos.[3] Neutrino masses could then depend upon the addition of 3 Dirac right-handed neutrinos. If we now adopt the phenomenological structure of D-brane models to describe the matter fields in the visible sector, then the model parameters of the cosmological set-up introduced herein could be (in principle) affected by the right-handed neutrinos, which would contribute to the total radiation energy density. For a decoupling temperature $\gtrsim$1 TeV, we have $g_*(T_{\rm dec}) \gtrsim 106.75$ and via (1) we find that the ν_R contribution to the non-SM relativistic energy density, $\Delta N_{\rm eff} \lesssim 0.14$, is well within the existing 95% CL upper limit. On the other hand, if ν_R's decouple near the QCD phase transition, a D-brane-like description of the matter fields in our cosmological setup can accommodate the larger value of $\Delta N_{\rm eff}$ derived using the helium abundance measurements of [78], while providing interesting predictions for LHC searches [127–129].

More concretely, in Fig. 8 we show the normalized posterior distributions of h_0 for different choices of $N_{\rm eff}$ from the 7 parameter fit of [130]. It is evident that the 95% CL limit on $\Delta N_{\rm eff}$ from the combination of CMB, BAO, and BBN observations [10] severely constrains a solution of the H_0 problem in terms of additional relativistic degrees of freedom. Consideration of the larger helium abundance measured in [78], with $\Delta N_{\rm eff} < 0.544$ at the 95% CL still precludes a full solution of the H_0 problem in terms of additional light species at the CMB epoch. However, the combined effect produced by fading dark matter and the extra relativistic degrees of freedom at the CMB epoch appears to have the potential to resolve the H_0 tension; see Fig. 8. A comprehensive study of the parameter space is beyond the scope of this paper and will be presented elsewhere. Needless to say, the helium abundance reported in [78] is in tension with Planck observations, so this solution would require a combination of two datasets which are in tension. On the one hand, the addition of extra relativistic degrees of freedom at the CMB epoch can accommodate the local calibration of SNe luminosities well out into the Hubble flow, avoiding the constraints of late times dark energy transitions [65]. On the other hand, we have noted that increasing the amount of radiation in the early universe leads to a higher value of S_8. Solutions that could mitigate this problem have been presented in [131].

Future experiments, such as CMBPol (which is expected to reach a 2σ precision of $\Delta N_{\rm eff} = 0.09$ [132]) and eventually CMB-S4 (which is expected to reach a 2σ

[3]However, it is possible that D-brane instantons can generate Majorana masses for these perturbatively forbidden operators [125,126].

precision of $\Delta N_{\rm eff} = 0.06$ [133]) will be able to probe the contributions from Υ's and ν_R's, providing additional constraints on the (extended) string cosmological set-up proposed in this section.

V. CONCLUSIONS

We have realized the Agrawal-Obied-Vafa swampland proposal of fading dark matter for relaxing the H_0 tension [63] by the model of Salam-Sezgin [66] and its string realization of Cvetič-Gibbons-Pope [67]. The model is fairly simple, it describes a compactification from six to four dimensions of a 6-dimensional SUGRA with a monopole background on a 2-sphere, allowing for time dependence of the 6-dimensional moduli fields while assuming a 4-dimensional metric with a Robertson-Walker form. In terms of linear combinations of the S^2 moduli field and the 6-dimensional dilaton, the 4-dimensional effective potential consists of a pure exponential function of a quintessence field Y which is the 4-dimensional dilaton and the field X which determines the 4-dimensional gauge couplings of NS5-branes. This avoids direct couplings of the dilaton to matter suppressing extra forces competing with gravity. It turns out that X is a source of CDM, with a mass proportional to an exponential function of the quintessence field. The asymptotic behavior of the Hubble parameter, $h \approx \ln t$, leads to a conformally flat Robertson-Walker metric for large times. The dS (vacuum) potential energy density is characterized by an exponential behavior $V_Y \propto e^{\sqrt{2}Y}$. Asymptotically, this represents the crossover situation with $w_Y = -1/3$, implying expansion at constant velocity with Y varying logarithmically $Y \approx -\ln t$ [68]. The deviation from constant velocity expansion into a brief accelerated phase encompassing the recent past ($z \lesssim 6$) makes the model phenomenologically viable.

We have shown that this set up is well equipped to reproduce the salient features of the AOV fading dark matter proposal. For $a = 0.178$, the model features a tower of light states X originating in the rolling of the Y field. These X particles constitute a portion of the CDM, and the way in which their mass evolve over time demonstrates that the model may help reducing (though not fully eliminate) the H_0 tension.

As a natural outgrowth of this work, we intend to study higher dimensional SUGRAs, which also admit monopole-like solutions [134]. In some cases, however, there are no compactifications to Minkowski vacuum [135]. Of particular interest is the gauged 8-dimensional SUGRA with matter couplings [136] where a solution of the form Minkowski$_6 \times S^2$ is known to exist. In addition, because the Salam-Sezgin model has $N = (1, 0)$ SUSY in 6 dimensions the $U(1)$ coupling is not fixed. In general it may be a combination of e^{ϕ} and $e^{-\phi}$ determined by chiral anomalies [137]. These may offer new possibilities for models of the type discussed in this paper. However, we remind the reader that late time dark energy transitions do not fully resolve the true source of tension between the distance ladder and high redshift observations [65] and therefore some additional assumptions (like those discussed in Sec. IV) must be adopted in order to solve the H_0 problem in the AOV-type string backgrounds.

In summary, the string cosmological framework put forward in this paper calls for new CMB observations and stimulates the investigation of complex theoretical models of the swampland as possible solutions of the H_0 problem.

ACKNOWLEDGMENTS

We thank Eleonora Di Valentino for some valuable discussion. The work of L. A. A. and J. F. S. is supported by the by the U.S. National Science Foundation (NSF Grant No. PHY-1620661) and the National Aeronautics and Space Administration (NASA Grant No. 80NSSC18K0464). The research of I. A. is funded in part by the Institute Lagrange de Paris, and in part by a CNRS PICS grant. The work of D. L. is supported by the Origins Excellence Cluster. The work of T. R. T is supported by NSF under Grant No. PHY1913328. Any opinions, findings, and conclusions or recommendations expressed in this material are those of the authors and do not necessarily reflect the views of the NSF or NASA.

APPENDIX

Since we have set to zero the fermionic terms in the background, the condition for the SUSY of the background is the vanishing of the supersymmetric variations of the fermionic fields; namely,

$$\delta\chi = \frac{\kappa}{2}(\partial_M \phi)\Gamma^M \epsilon + \frac{1}{12} e^{-\phi} G_{MNP}\Gamma^{MNP}\epsilon = 0, \quad \text{(A1)}$$

$$\delta\lambda = \frac{1}{2\sqrt{2}} e^{-\phi/2} F_{MN}\Gamma^{MN}\epsilon - \frac{i}{\sqrt{2}} g e^{-\phi/2}\epsilon = 0, \quad \text{(A2)}$$

and

$$\delta\psi_M = \frac{1}{\kappa}\mathcal{D}_M \epsilon + \frac{1}{24} e^{-\phi} G_{PQR}\Gamma^{PQR}\Gamma_M \epsilon = 0, \quad \text{(A3)}$$

for the axino, the dilatino, and the gravitino; respectively [66]. Here, $\Gamma^{PQR} = \Gamma^{[P}\Gamma^{Q}\Gamma^{R]}$ is the fully antisymmetric product of three Γ-matrices of the 6-dimensional Clifford algebra. The covariant derivative of the gravitino,

$$\mathcal{D}_M \psi_N = \left(\partial_M + \frac{1}{4}\omega_{MAB}\Gamma^{AB} - igA_M\right)\psi_N, \quad \text{(A4)}$$

is given in terms of the torsionfree spin connection ω_M^{AB}. (The Christoffel connection is not needed because of the contraction with the antisymmetric gamma-matrix.) Using the vielbein e_A^M, we have

$$\omega_M^{AB} = 2e^{N[A}\partial_{[M}e_{N]}{}^{B]} - e^{N[A}e^{B]P}e_{MC}\partial_N e_P^C. \quad \text{(A5)}$$

In familiar notation: $\Gamma_\mu = \gamma_\mu \times \sigma^1$, $\Gamma_5 = \gamma_5 \times \sigma^1$, $\Gamma_6 = \mathbb{1} \times \sigma^2$, $\{\Gamma_M, \Gamma_N\} = 2\eta_{MN}$, $\gamma_5^2 = \mathbb{1}$ and so $\Gamma_{56} = \gamma_5 \times i\sigma^3$ and $\Gamma_7 = \Gamma_0\Gamma_1\cdots\Gamma_6 = \mathbb{1} \times \sigma^3$ [138].

With this in mind, the nonzero components of the spin connection are found to be $\omega_{\hat{i}}^{i0} = e^h(\dot{f} + \dot{h})$, $\omega_{\hat{5}}^{05} = r_c\dot{f}$, $\omega_{\hat{6}}^{06} = r_c\dot{f}\sin\vartheta$, $\omega_{\hat{6}}^{56} = \cos\vartheta$, where we adopted the also familiar notation of carets on the curved indices (which are lowered or raised with the spacetime metric g_{MN}) to distinguish them from the flat indices (that are lowered or raised with the flat Minkowski metric η_{AB}), so that $g^{MN} = \eta^{AB}e_A^M e_B^N$; lowercase latin indices are used for the 3 spatial components of M_4, and run from 1 to 3. The contraction $F_{MN}\Gamma^{MN}$ in (A2) takes the form

$$F_{MN}\Gamma^{MN} = 2F_{\hat{5}\hat{6}}\Gamma^{\hat{5}\hat{6}} = 2b\,\sin\vartheta e_{\hat{5}}^{\hat{5}}e_{\hat{6}}^{\hat{6}}\Gamma^{56} = 2\frac{b}{r_c^2}e^{-2f}\Gamma_{56}. \quad \text{(A6)}$$

Substituting (A6) into (A2) we obtain

$$\frac{1}{\sqrt{2}}e^{-\phi/2}[be^{-2f}\Gamma_{56}\epsilon - ige^{\phi}\epsilon] = 0. \quad \text{(A7)}$$

Remarkably, the field equations fixed the monopole charged to be ± 1, and lead to the condition [66]

$$\Gamma_{56}\epsilon = \pm i\epsilon. \quad \text{(A8)}$$

Using (A8) we rewrite (A7) as

$$e^{2f+\phi} = \pm\frac{b}{g}. \quad \text{(A9)}$$

In a similar fashion, $\delta\psi_{\hat{0}} = 0$ leads to

$$\partial_0\epsilon = 0, \quad \text{(A10)}$$

from which we conclude that ϵ is not a function of t. The condition $\delta\psi_{\hat{i}} = 0$ yields

$$\partial_i\epsilon + \frac{1}{2}\omega_{\hat{i}}^{i0}\Gamma_{i0}\epsilon = \partial_i\epsilon + \frac{1}{2}e^h(\dot{f} + \dot{h})\Gamma_{i0}\epsilon = 0, \quad \text{(A11)}$$

and $\delta\psi_{\hat{5}} = 0$ gives

$$\partial_5\epsilon + \frac{1}{2}\omega_{\hat{5}}^{50}\Gamma_{50}\epsilon - igA_{\hat{5}}\epsilon = \partial_5\epsilon + \frac{1}{2}r_c\dot{f}\Gamma_{50}\epsilon = 0. \quad \text{(A12)}$$

Next, $\delta\psi_{\hat{6}} = 0$, leads to

$$\partial_6\epsilon + \frac{1}{2}\omega_{\hat{6}}^{60}\Gamma_{60}\epsilon + \frac{1}{2}\omega_{\hat{6}}^{56}\Gamma_{56}\epsilon - igA_6\epsilon = 0, \quad \text{(A13)}$$

which translates into

$$\partial_6\epsilon + \frac{1}{2}r_c\dot{f}\sin\vartheta\Gamma_{60}\epsilon = 0 \quad \text{(A14)}$$

and

$$\frac{1}{2}\cos\vartheta\Gamma_{56}\epsilon - igb\cos\vartheta\epsilon = 0. \quad \text{(A15)}$$

Substituting the relation $g = \sqrt{\xi}/2$ into (A15) while imposing (A8) we obtain the constraint $b^2\xi = 1$. Finally, the variation of $\delta\chi$ implies

$$\frac{\kappa}{2}\partial_0\phi\Gamma_{\hat{0}}\epsilon = 0, \quad \text{(A16)}$$

which sets $\dot{\phi} = 0$.

The constraints from imposing the SUSY background can be summarized as follows: the relation (A16) demands ϕ to be a constant and when this condition is combined with (A9) we see that f must also be a constant. Because f is a constant, we can immediately see by inspection of (A10), (A12), and (A14) that ϵ is independent of both t and the coordinates of the compact space ϑ and φ. Likewise, we rewrite (A11) as

$$\partial_i\epsilon + \frac{1}{2}e^h\dot{h}\Gamma_{i0}\epsilon = 0. \quad \text{(A17)}$$

The temporal dependence of (A17) then becomes

$$e^h\dot{h} = \varkappa_1, \quad \text{(A18)}$$

and so the scale factor for a SUSY background is found to be

$$e^h = \varkappa_1 t + \varkappa_2, \quad \text{(A19)}$$

with $\varkappa_1$ and $\varkappa_2$ constants.

[1] W. L. Freedman, Cosmology at a crossroads, Nat. Astron. **1**, 0121 (2017).

[2] A. G. Riess, L. Macri, S. Casertano, H. Lampeitl, H. C. Ferguson, A. V. Filippenko, S. W. Jha, W. Li, and R. Chornock, A 3% solution: Determination of the Hubble constant with the Hubble space telescope and wide field camera 3, Astrophys. J. **730**, 119 (2011); **732**, 129(E) (2011).

[3] A. G. Riess *et al.*, A 2.4% determination of the local value of the Hubble constant, Astrophys. J. **826**, 56 (2016).

[4] A. G. Riess *et al.*, Milky Way Cepheid standards for measuring cosmic distances and application to Gaia DR2: Implications for the Hubble constant, Astrophys. J. **861**, 126 (2018).

[5] V. Bonvin *et al.*, H0LiCOW V. New Cosmograil time delays of HE 0435-1223: H_0 to 3.8 per cent precision from

strong lensing in a flat ΛCDM model, Mon. Not. R. Astron. Soc. **465**, 4914 (2017).
[6] S. Birrer *et al.*, H0LiCOW - IX. Cosmographic analysis of the doubly imaged quasar SDSS 1206 + 4332 and a new measurement of the Hubble constant, Mon. Not. R. Astron. Soc. **484**, 4726 (2019).
[7] A. G. Riess, S. Casertano, W. Yuan, L. M. Macri, and D. Scolnic, Large Magellanic Cloud Cepheid standards provide a 1% foundation for the determination of the Hubble constant and stronger evidence for physics beyond ΛCDM, Astrophys. J. **876**, 85 (2019).
[8] G. Hinshaw *et al.* (WMAP Collaboration), Nine-year Wilkinson Microwave Anisotropy Probe (WMAP) observations: Cosmological parameter results, Astrophys. J. Suppl. Ser. **208**, 19 (2013).
[9] P. A. R. Ade *et al.* (Planck Collaboration), Planck 2015 results XIII: Cosmological parameters, Astron. Astrophys. **594**, A13 (2016).
[10] N. Aghanim *et al.* (Planck Collaboration), Planck 2018 results VI: Cosmological parameters, arXiv:1807.06209.
[11] L. Verde, T. Treu, and A. G. Riess, Tensions between the early and the late universe, Nat. Astron. **3**, 891 (2019).
[12] B. Follin and L. Knox, Insensitivity of the distance ladder Hubble constant determination to Cepheid calibration modelling choices, Mon. Not. R. Astron. Soc. **477**, 4534 (2018).
[13] S. Dhawan, S. W. Jha, and B. Leibundgut, Measuring the Hubble constant with type Ia supernovae as near-infrared standard candles, Astron. Astrophys. **609**, A72 (2018).
[14] T. Shanks, L. Hogarth, and N. Metcalfe, Gaia Cepheid parallaxes and "local hole" relieve H_0 tension, Mon. Not. R. Astron. Soc. **484**, L64 (2019).
[15] A. G. Riess, S. Casertano, D. Kenworthy, D. Scolnic, and L. Macri, Seven problems with the claims related to the Hubble tension in arXiv:1810.02595, Mon. Not. R. Astron. Soc. **484**, L64 (2019).
[16] C. A. P. Bengaly, U. Andrade, and J. S. Alcaniz, How does an incomplete sky coverage affect the Hubble constant variance? Eur. Phys. J. C **79**, 768 (2019).
[17] M. Rameez and S. Sarkar, Is there really a 'Hubble tension'? arXiv:1911.06456.
[18] C. Vafa, The String landscape and the swampland, arXiv:hep-th/0509212.
[19] N. Arkani-Hamed, L. Motl, A. Nicolis, and C. Vafa, The string landscape, black holes and gravity as the weakest force, J. High Energy Phys. 06 (2007) 060.
[20] H. Ooguri and C. Vafa, On the geometry of the string landscape and the Swampland, Nucl. Phys. **B766**, 21 (2007).
[21] D. Klaewer and E. Palti, Super-Planckian spatial field variations and quantum gravity, J. High Energy Phys. 01 (2017) 088.
[22] H. Ooguri and C. Vafa, Non-supersymmetric AdS and the swampland, Adv. Theor. Math. Phys. **21**, 1787 (2017).
[23] E. Palti, The weak gravity conjecture and scalar fields, J. High Energy Phys. 08 (2017) 034.
[24] G. Obied, H. Ooguri, L. Spodyneiko, and C. Vafa, de Sitter space and the swampland, arXiv:1806.08362.
[25] D. Andriot, On the de Sitter swampland criterion, Phys. Lett. B **785**, 570 (2018).
[26] S. Cecotti and C. Vafa, Theta-problem and the string swampland, arXiv:1808.03483.
[27] S. K. Garg and C. Krishnan, Bounds on slow roll and the de Sitter swampland, J. High Energy Phys. 11 (2019) 075.
[28] H. Ooguri, E. Palti, G. Shiu, and C. Vafa, Distance and de Sitter conjectures on the swampland, Phys. Lett. B **788**, 180 (2019).
[29] D. Klaewer, D. Lüst, and E. Palti, A spin2 conjecture on the swampland, Fortschr. Phys. **67**, 1800102 (2019).
[30] J. J. Heckman and C. Vafa, Fine tuning, sequestering, and the swampland, Phys. Lett. B **798**, 135004 (2019).
[31] D. Lüst, E. Palti, and C. Vafa, AdS and the swampland, Phys. Lett. B **797**, 134867 (2019).
[32] A. Bedroya and C. Vafa, Trans-Planckian censorship and the swampland, arXiv:1909.11063.
[33] A. Kehagias, D. Lüst, and S. Lüst, Swampland, gradient flow and infinite distance, arXiv:1910.00453.
[34] R. Blumenhagen, M. Brinkmann, and A. Makridou, Quantum log-corrections to Swampland conjectures, J. High Energy Phys. 02 (2020) 064.
[35] T. D. Brennan, F. Carta, and C. Vafa, The string landscape, the swampland, and the missing corner, *Proc. Sci.*, TASI2017 (2017) 015 [arXiv:1711.00864].
[36] E. Palti, The Swampland: introduction and review, Fortschr. Phys. **67**, 1900037 (2019).
[37] T. W. Grimm, E. Palti, and I. Valenzuela, Infinite distances in field space and massless towers of states, J. High Energy Phys. 08 (2018) 143.
[38] B. Heidenreich, M. Reece, and T. Rudelius, Emergence of Weak Coupling at Large Distance in Quantum Gravity, Phys. Rev. Lett. **121**, 051601 (2018).
[39] S. Laliberte and R. Brandenberger, String gases and the Swampland, arXiv:1911.00199.
[40] R. Bousso, A covariant entropy conjecture, J. High Energy Phys. 07 (1999) 004.
[41] R. Bousso, B. Freivogel, and I. S. Yang, Eternal inflation: The inside story, Phys. Rev. D **74**, 103516 (2006).
[42] P. Agrawal, G. Obied, P. J. Steinhardt, and C. Vafa, On the cosmological implications of the string swampland, Phys. Lett. B **784**, 271 (2018).
[43] E. Di Valentino, A. Melchiorri, and J. Silk, Reconciling Planck with the local value of H_0 in extended parameter space, Phys. Lett. B **761**, 242 (2016).
[44] E. Di Valentino, A. Melchiorri, E. V. Linder, and J. Silk, Constraining dark energy dynamics in extended parameter space, Phys. Rev. D **96**, 023523 (2017).
[45] V. Poulin, T. L. Smith, T. Karwal, and M. Kamionkowski, Early Dark Energy Can Resolve the Hubble Tension, Phys. Rev. Lett. **122**, 221301 (2019).
[46] N. Kaloper, Dark energy, H_0 and weak gravity conjecture, Int. J. Mod. Phys. D **28**, 1944017 (2019).
[47] P. Agrawal, F. Y. Cyr-Racine, D. Pinner, and L. Randall, Rock 'n' Roll solutions to the Hubble tension, arXiv:1904.01016.
[48] J. Sakstein and M. Trodden, Early dark energy from massive neutrinos—A natural resolution of the Hubble tension, arXiv:1911.11760 [Phys. Rev. Lett. (to be published)].
[49] P. A. R. Ade *et al.* (Planck Collaboration), Planck 2013 results XX: Cosmology from SunyaevZeldovich cluster counts, Astron. Astrophys. **571**, A20 (2014).

[50] T. M. C. Abbott *et al.* (DES Collaboration), Dark energy survey year 1 results: Cosmological constraints from galaxy clustering and weak lensing, Phys. Rev. D **98**, 043526 (2018).
[51] H. Hildebrandt *et al.*, KiDS-450: Cosmological parameter constraints from tomographic weak gravitational lensing, Mon. Not. R. Astron. Soc. **465**, 1454 (2017).
[52] J. C. Hill, E. McDonough, M. W. Toomey, and S. Alexander, Early dark energy does not restore cosmological concordance, arXiv:2003.07355.
[53] V. Salvatelli, N. Said, M. Bruni, A. Melchiorri, and D. Wands, Indications of a Late-Time Interaction in the Dark Sector, Phys. Rev. Lett. **113**, 181301 (2014).
[54] J. Vliviita and E. Palmgren, Distinguishing interacting dark energy from wCDM with CMB, lensing, and baryon acoustic oscillation data, J. Cosmol. Astropart. Phys. 07 (2015) 015.
[55] E. G. M. Ferreira, J. Quintin, A. A. Costa, E. Abdalla, and B. Wang, Evidence for interacting dark energy from BOSS, Phys. Rev. D **95**, 043520 (2017).
[56] R. Murgia, S. Gariazzo, and N. Fornengo, Constraints on the coupling between dark energy and dark matter from CMB data, J. Cosmol. Astropart. Phys. 04 (2016) 014.
[57] S. Kumar and R. C. Nunes, Echo of interactions in the dark sector, Phys. Rev. D **96**, 103511 (2017).
[58] E. Di Valentino, A. Melchiorri, and O. Mena, Can interacting dark energy solve the H_0 tension? Phys. Rev. D **96**, 043503 (2017).
[59] W. Yang, S. Pan, E. Di Valentino, R. C. Nunes, S. Vagnozzi, and D. F. Mota, Tale of stable interacting dark energy, observational signatures, and the H_0 tension, J. Cosmol. Astropart. Phys. 09 (2018) 019.
[60] S. Kumar, R. C. Nunes, and S. K. Yadav, Dark sector interaction: A remedy of the tensions between CMB and LSS data, Eur. Phys. J. C **79**, 576 (2019).
[61] E. Di Valentino, A. Melchiorri, O. Mena, and S. Vagnozzi, Interacting dark energy after the latest Planck, DES, and H_0 measurements: An excellent solution to the H_0 and cosmic shear tensions, arXiv:1908.04281.
[62] E. Di Valentino, A. Melchiorri, O. Mena, and S. Vagnozzi, Nonminimal dark sector physics and cosmological tensions, Phys. Rev. D **101**, 063502 (2020).
[63] P. Agrawal, G. Obied, and C. Vafa, H_0 tension, Swampland conjectures and the epoch of fading dark matter, arXiv:1906.08261.
[64] C. Vafa, Cosmic predictions from the string swampland, Physics **12**, 115 (2019).
[65] G. Benevento, W. Hu, and M. Raveri, Can late dark energy transitions raise the Hubble constant? arXiv:2002.11707.
[66] A. Salam and E. Sezgin, Chiral compactification on Minkowski $\times S^2$ of $N = 2$ Einstein-Maxwell supergravity in six-dimensions, Phys. Lett. **147B**, 47 (1984).
[67] M. Cvetič, G. W. Gibbons, and C. N. Pope, A string and M theory origin for the Salam-Sezgin model, Nucl. Phys. **B677**, 164 (2004).
[68] I. Antoniadis, C. Bachas, J. R. Ellis, and D. V. Nanopoulos, Cosmological string theories and discrete inflation, Phys. Lett. B **211**, 393 (1988); An expanding universe in string theory, Nucl. Phys. **B328**, 117 (1989).
[69] L. Anchordoqui, H. Goldberg, S. Nawata, and C. Nuñez, Cosmology from string theory, Phys. Rev. D **76**, 126005 (2007).
[70] G. Steigman, D. N. Schramm, and J. E. Gunn, Cosmological limits to the number of massive leptons, Phys. Lett. B **66**, 202 (1977).
[71] G. Mangano, G. Miele, S. Pastor, T. Pinto, O. Pisanti, and P. D. Serpico, Relic neutrino decoupling including flavor oscillations, Nucl. Phys. **B729**, 221 (2005).
[72] E. W. Kolb and M. S. Turner, The early universe, Front. Phys. **69**, 1 (1990).
[73] E. Aver, K. A. Olive, and E. D. Skillman, The effects of He I λ10830 on helium abundance determinations, J. Cosmol. Astropart. Phys. 07 (2015) 011.
[74] A. Peimbert, M. Peimbert, and V. Luridiana, The primordial helium abundance and the number of neutrino families, Rev. Mex. Astron. Astrofis. **52**, 419 (2016).
[75] R. J. Cooke, M. Pettini, and C. C. Steidel, One percent determination of the primordial deuterium abundance, Astrophys. J. **855**, 102 (2018).
[76] O. Pisanti, A. Cirillo, S. Esposito, F. Iocco, G. Mangano, G. Miele, and P. D. Serpico, PArthENoPE: Public algorithm evaluating the nucleosynthesis of primordial elements, Comput. Phys. Commun. **178**, 956 (2008).
[77] L. E. Marcucci, G. Mangano, A. Kievsky, and M. Viviani, Implication of the Proton-Deuteron Radiative Capture for Big Bang Nucleosynthesis, Phys. Rev. Lett. **116**, 102501 (2016); **117**, 049901(E) (2016).
[78] Y. I. Izotov, T. X. Thuan, and N. G. Guseva, A new determination of the primordial He abundance using the He I λ10830 Å emission line: cosmological implications, Mon. Not. R. Astron. Soc. **445**, 778 (2014).
[79] E. Ó Colgáin, M. H. P. M. van Putten, and H. Yavartanoo, de Sitter Swampland, H_0 tension and observation, Phys. Lett. B **793**, 126 (2019).
[80] L. Heisenberg, M. Bartelmann, R. Brandenberger, and A. Refregier, Dark energy in the swampland, Phys. Rev. D **98**, 123502 (2018).
[81] Y. Akrami, R. Kallosh, A. Linde, and V. Vardanyan, The landscape, the swampland and the era of precision cosmology, Fortschr. Phys. **67**, 1800075 (2019).
[82] C. I. Chiang, J. M. Leedom, and H. Murayama, What does inflation say about dark energy given the swampland conjectures? Phys. Rev. D **100**, 043505 (2019).
[83] M. Raveri, W. Hu, and S. Sethi, Swampland conjectures and late-time cosmology, Phys. Rev. D **99**, 083518 (2019).
[84] E. Elizalde and M. Khurshudyan, Swampland criteria for a dark energy dominated universe ensuing from Gaussian processes and H(z) data analysis, Phys. Rev. D **99**, 103533 (2019).
[85] S. Brahma and M. W. Hossain, Dark energy beyond quintessence: Constraints from the swampland, J. High Energy Phys. 06 (2019) 070.
[86] E. Ó Colgáin and H. Yavartanoo, Testing the swampland: H_0 tension, arXiv:1905.02555.
[87] I. Baldes, D. Chowdhury, and M. H. G. Tytgat, Forays into the dark side of the swamp, Phys. Rev. D **100**, 095009 (2019).
[88] P. Brax, C. van de Bruck, and A. C. Davis, The swampland and screened modified gravity, arXiv:1911.09169.

[89] W. Yang, M. Shahalam, B. Pal, S. Pan, and A. Wang, Constraints on quintessence scalar field models using cosmological observations, Phys. Rev. D **100**, 023522 (2019).

[90] F. Tosone, B. S. Haridasu, V. V. Lukovi, and N. Vittorio, Constraints on field flows of quintessence dark energy, Phys. Rev. D **99**, 043503 (2019).

[91] A. Achúcarro and G. A. Palma, The string swampland constraints require multi-field inflation, J. Cosmol. Astropart. Phys. 02 (2019) 041.

[92] A. Kehagias and A. Riotto, A note on inflation and the swampland, Fortschr. Phys. **66**, 1800052 (2018).

[93] H. Matsui and F. Takahashi, Eternal inflation and swampland conjectures, Phys. Rev. D **99**, 023533 (2019).

[94] I. Ben-Dayan, Draining the swampland, Phys. Rev. D **99**, 101301 (2019).

[95] W. H. Kinney, S. Vagnozzi, and L. Visinelli, The zoo plot meets the swampland: Mutual (in)consistency of single-field inflation, string conjectures, and cosmological data, Classical Quantum Gravity **36**, 117001 (2019).

[96] O. Aharony, M. Berkooz, D. Kutasov, and N. Seiberg, Linear dilatons, NS five-branes and holography, J. High Energy Phys. 10 (1998) 004.

[97] R. M. Wald, *General Relativity* (University of Chicago Press, Chicago, 1984).

[98] J. Vinet and J. M. Cline, Codimension-two branes in six-dimensional supergravity and the cosmological constant problem, Phys. Rev. D **71**, 064011 (2005).

[99] S. M. Carroll, Quintessence and the Rest of the World, Phys. Rev. Lett. **81**, 3067 (1998).

[100] T. R. Taylor and G. Veneziano, Dilaton couplings at large distances, Phys. Lett. B **213**, 450 (1988).

[101] See e.g. E. G. Adelberger, Torsion-balance probes of fundamental physics, arXiv:1308.3213, and references therein.

[102] I. Antoniadis, S. Dimopoulos, and A. Giveon, Little string theory at a TeV, J. High Energy Phys. 05 (2001) 055.

[103] L. Anchordoqui and H. Goldberg, Time variation of the fine structure constant driven by quintessence, Phys. Rev. D **68**, 083513 (2003).

[104] M. S. Turner, Coherent scalar field oscillations in an expanding Universe, Phys. Rev. D **28**, 1243 (1983).

[105] P. J. Steinhardt, L. M. Wang, and I. Zlatev, Cosmological tracking solutions, Phys. Rev. D **59**, 123504 (1999).

[106] U. Franca and R. Rosenfeld, Fine tuning in quintessence models with exponential potentials, J. High Energy Phys. 10 (2002) 015.

[107] T. M. C. Abbott *et al.* (DES Collaboration), Cosmological Constraints from Multiple Probes in the Dark Energy Survey, Phys. Rev. Lett. **122**, 171301 (2019).

[108] T. M. C. Abbott *et al.* (DES Collaboration), First cosmology results using type Ia supernovae from the dark energy survey: Constraints on cosmological parameters, Astrophys. J. **872**, L30 (2019).

[109] M. Tanabashi *et al.* (Particle Data Group), Review of particle physics, Phys. Rev. D **98**, 030001 (2018).

[110] O. Farooq, F. R. Madiyar, S. Crandall, and B. Ratra, Hubble parameter measurement constraints on the redshift of the decelerationacceleration transition, dynamical dark energy, and space curvature, Astrophys. J. **835**, 26 (2017).

[111] J. Simon, L. Verde, and R. Jimenez, Constraints on the redshift dependence of the dark energy potential, Phys. Rev. D **71**, 123001 (2005).

[112] J. L. Sievers *et al.* (Atacama Cosmology Telescope Collaboration), The Atacama cosmology telescope: Cosmological parameters from three seasons of data, J. Cosmol. Astropart. Phys. 10 (2013) 060.

[113] M. Moresco *et al.*, Improved constraints on the expansion rate of the Universe up to $z \sim 1.1$ from the spectroscopic evolution of cosmic chronometers, J. Cosmol. Astropart. Phys. 08 (2012) 006.

[114] C. Zhang, H. Zhang, S. Yuan, T. J. Zhang, and Y. C. Sun, Four new observational $H(z)$ data from luminous red galaxies in the Sloan Digital Sky Survey data release seven, Res. Astron. Astrophys. **14**, 1221 (2014).

[115] A. Font-Ribera *et al.* (BOSS Collaboration), Quasar-Lyman α forest cross-correlation from BOSS DR11: Baryon acoustic oscillations, J. Cosmol. Astropart. Phys. 05 (2014) 027.

[116] T. Delubac *et al.* (BOSS Collaboration), Baryon acoustic oscillations in the Lyα forest of BOSS DR11 quasars, Astron. Astrophys. **574**, A59 (2015).

[117] M. Moresco, Raising the bar: New constraints on the Hubble parameter with cosmic chronometers at $z \sim 2$, Mon. Not. R. Astron. Soc. **450**, L16 (2015).

[118] M. Moresco, Lucia Pozzetti, Andrea Cimatti, Raul Jimenez, Claudia Maraston, Licia Verde, Daniel Thomas, Annalisa Citro, Rita Tojeiro, and David Wilkinson, A 6% measurement of the Hubble parameter at $z \sim 0.45$: Direct evidence of the epoch of cosmic re-acceleration, J. Cosmol. Astropart. Phys. 05 (2016) 014.

[119] C. Blake *et al.*, The WiggleZ dark energy Survey: Joint measurements of the expansion and growth history at $z < 1$, Mon. Not. R. Astron. Soc. **425**, 405 (2012).

[120] S. Alam *et al.* (BOSS Collaboration), The clustering of galaxies in the completed SDSS-III Baryon Oscillation Spectroscopic Survey: Cosmological analysis of the DR12 galaxy sample, Mon. Not. R. Astron. Soc. **470**, 2617 (2017).

[121] D. Lüst, Intersecting brane worlds: A path to the standard model? Classical Quantum Gravity **21**, S1399 (2004).

[122] R. Blumenhagen, M. Cvetič, P. Langacker, and G. Shiu, Toward realistic intersecting D-brane models, Annu. Rev. Nucl. Part. Sci. **55**, 71 (2005).

[123] R. Blumenhagen, B. Kors, D. Lüst, and S. Stieberger, Four-dimensional string compactifications with D-Branes, orientifolds and fluxes, Phys. Rep. **445**, 1 (2007).

[124] S. Weinberg, Varieties of baryon and lepton nonconservation, Phys. Rev. D **22**, 1694 (1980).

[125] R. Blumenhagen, M. Cvetic, and T. Weigand, Spacetime instanton corrections in 4D string vacua: The seesaw mechanism for D-brane models, Nucl. Phys. **B771**, 113 (2007).

[126] L. E. Ibanez and A. M. Uranga, Neutrino Majorana masses from string theory instanton effects, J. High Energy Phys. 03 (2007) 052.

[127] L. A. Anchordoqui and H. Goldberg, Neutrino Cosmology after WMAP 7-Year Data and LHC First Z' Bounds, Phys. Rev. Lett. **108**, 081805 (2012).

[128] L. A. Anchordoqui, I. Antoniadis, H. Goldberg, X. Huang, D. Lüst, T. R. Taylor, and B. Vlcek, LHC phenomenology and cosmology of string-inspired intersecting D-brane models, Phys. Rev. D **86**, 066004 (2012).

[129] L. A. Anchordoqui, H. Goldberg, and G. Steigman, Right-handed neutrinos as the dark radiation: Status and forecasts for the LHC, Phys. Lett. B **718**, 1162 (2013).

[130] S. Vagnozzi, New physics in light of the H_0 tension: An alternative view, arXiv:1907.07569.

[131] E. Di Valentino and S. Bridle, Exploring the tension between current cosmic microwave background and cosmic shear data, Symmetry **10**, 585 (2018).

[132] S. Galli, M. Martinelli, A. Melchiorri, L. Pagano, B. D. Sherwin, and D. N. Spergel, Constraining fundamental physics with future CMB experiments, Phys. Rev. D **82**, 123504 (2010).

[133] K. Abazajian *et al.*, CMB-S4 science case, reference design, and project plan, arXiv:1907.04473.

[134] A. Salam and E. Sezgin, *Supergravities in Diverse Dimensions* (Elsevier, North-Holland, 1989), Vol. 1 and 2.

[135] A. Salam and E. Sezgin, $D = 8$ supergravity, Nucl. Phys. **B258**, 284 (1985).

[136] A. Salam and E. Sezgin, $D = 8$ supergravity: Matter couplings, gauging and Minkowski compactification, Phys. Lett. **154B**, 37 (1985).

[137] N. Seiberg and E. Witten, Comments on string dynamics in six-dimensions, Nucl. Phys. **B471**, 121 (1996).

[138] S. Randjbar-Daemi, A. Salam, and J. A. Strathdee, Spontaneous compactification in six-dimensional Einstein-Maxwell theory, Nucl. Phys. **B214**, 491 (1983).